Simulation of NDT Inspection in 3D Elastic Waveguide Involving Arbitrary Defect

Vahan BARONIAN [1], Karim JEZZINE [2]
[1] CEA LIST, Gif-sur-Yvette, France
[2] CEA LIST, Toulouse, France

Contact e-mail: vahan.baronian@cea.fr

Abstract. Models for ultrasonic guided wave NDT are developed at CEA LIST and integrated into the CIVA software platform. Plates, cylinders, guides of arbitrary cross section, possibly multi-layered, may be addressed. Mode computation, radiated field from different type of transducers (contact with or without wedge, surrounding or surrounded arrays in pipes) and response of a NDT examination in pulse-echo or pitch-catch configurations are proposed.

The latter simulation requires a model to compute the interaction of guided waves by any perturbation (cracks, inclusions and topological variations). Such a numerical method based on a coupling with Modal and Finite Elements representation has been integrated in CIVA 11 GWT (released in 2014), but only for the cases of 2D (in planar guides) or axisymmetric perturbations (in cylinders).

In CIVA 2016 release, this method will be implemented for the computation of the scattering by any perturbation in 3D elastic waveguide.

The aim of this paper is to show the new capabilities offered by CIVA for the simulation of NDT experiment by guided waves. A numerical study on the scattering by cracks at different locations in rails will be shown.

Introduction

Simulation tools for guided wave inspections may help to design and optimise NDT methods or probes, or to interpret experimental data. Models developed in the CIVA software platform [1] are based on a modal decomposition. Modes propagating in a waveguide may be transmitted through or reflected on a guide discontinuity or converted into other modes. Simulations are thus performed in the frequency domain and are subsequently synthesized by Fourier transform over the transducer frequency bandwidth.

At a given frequency, the elastodynamic field (particle displacement or velocity, stress) in a straight waveguide can be decomposed as a linear combination of eigenmodes computed in the cross-section of the structure. If the guide axis is x_3, a mode is defined at a given frequency by its wavenumber β_n and its particle displacement vector $\boldsymbol{u^n}(\boldsymbol{x_S})$ in the cross-section of the waveguide. $\boldsymbol{x_S}$ denotes the position in the cross section. The displacement $\boldsymbol{u}(\boldsymbol{x};t)$ at any position $\boldsymbol{x} = (\boldsymbol{x_S}, x_3)$ in the waveguide at the pulsation ω is expressed by:

$$\boldsymbol{u}(\boldsymbol{x};t) = \sum_n A_n \, \boldsymbol{u^n}(\boldsymbol{x_S}) e^{-j(\beta_n x_3 - \omega t)}$$

where A_n denotes the n^{th} amplitude coefficient in the decomposition.

A given mode may be transmitted through or reflected on a guide discontinuity or partially converted into other modes. The modal description is used in the regular parts of the waveguide, whereas models for transduction or scattering by guide discontinuities or flaws are used locally. To compute modal solutions, the semi-analytical finite element method has been implemented. This method allows the computation of both wavenumbers β_n, and modal displacements $\boldsymbol{u^n}(\boldsymbol{x_S})$. It can deal with waveguides of arbitrary section and anisotropic materials.

In presence of a local guide discontinuity or a flaw, the scattering problem is written in the form of a matrix of complex coefficients R_{nm} and T_{nm}. R_{nm} (resp. T_{nm}) is the reflection (resp. transmission) coefficient for the incident m^{th} mode and the reflected (resp. transmitted) n^{th} mode.

In this paper, the modelling approach used in CIVA for the simulation of GW inspections is presented. Applications to rail inspections are shown.

1 Hybrid SAFE-FE modelling

1.1 Mode computation and account of transducers

The computation of wavenumbers and modal displacements in a regular waveguide is performed thanks to the semi-analytical finite element method (SAFE) [2]. Wavenumbers and modal displacements correspond to eigenvalues and eigenvectors of a quadratic system of equations. Multilayered structures, anisotropy and viscoelasticity can be accounted for. Guide section is meshed either by 1D linear element for plates, cylinders or tubes, or 6-noded triangular finite elements in the case of arbitrary section, such as a rail.

The computation of modal amplitudes emitted by a transducer may be performed under the assumption that piezo-transducers can be modelled as sources of normal or tangential stresses over their active surface. For a transducer acting from the guiding surface, a Green function for a given mode is derived and a surface integration over the transducer performed [3].

1.2 Computation of scattering matrix for flaw interaction

To deal with arbitrary flaw shapes, guide inhomogeneities or junctions between several guides, a finite element (FE) scheme has been developed with the further goal to limit the computation zone to a minimal size for efficiency. The computation relies on the use of artificial boundary conditions endowing transparency on the FE box boundaries. These conditions are expressed in terms of the so called mixed vectors X and Y [4]. Radiation conditions at infinity are brought back to the artificial boundaries by building an operator coupling the finite elements to modal solutions in guides. An original mixed formulation has been derived whose unknowns are the displacement field in the bounded domain and the normal component of the normal stresses on the artificial boundaries. The scattered field is then projected on modal solutions in guides through the use of bi-orthogonality relations. This hybrid Modal-FE model has been established for 2D (Lamb modes) and 3D

waveguides in Cartesians coordinates. The theoretical details of this method are not given here but can be found in [5].

1.3 Simulation of a complete NDT inspection

A simulation of guided wave inspection through a taper junction between two different pipes is illustrated on Figure 1. The mesh of FE zone is represented and the corresponding transparent boundaries are also shown. Once the modal solution on each side of the guide discontinuity is obtained for the frequencies of interest, the modal amplitudes emitted by the transducer and the scattering matrix of the defect R_{nm} or T_{nm} can be computed separately and then combined to get the electrical signal $s(\omega)$ recorded by the receiver in the presence of the perturbation. The expression of $s(\omega)$ involving the various terms is presented on Figure 1. Standard Fourier synthesis is further applied to predict time-dependent waveforms (A-scan) typical of those measured in practice [6].

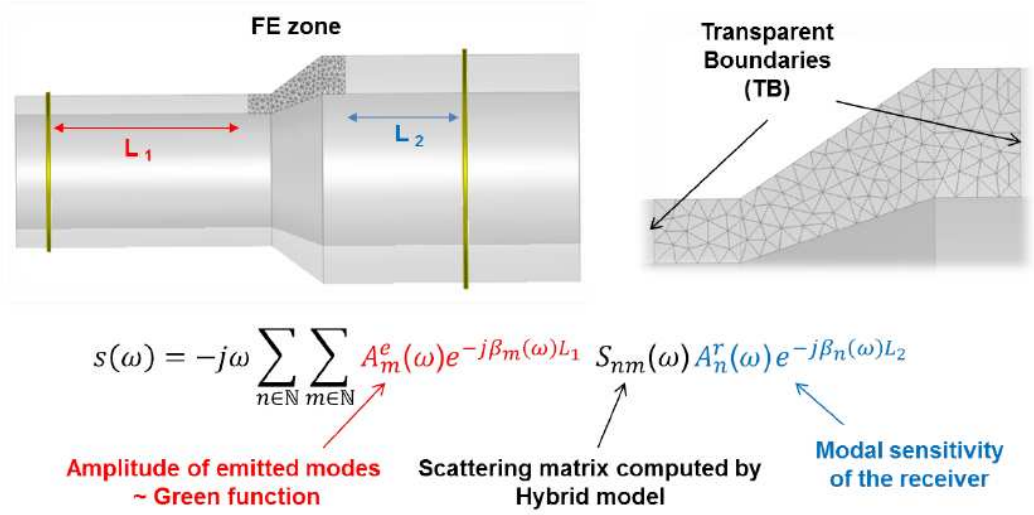

Fig. 1. Simulation of GW inspection of a taper junction using hybrid modal/FE model. (Left) Surrounding arrays probes configuration and sketch of the FE zone corresponding to the taper junction. (Right) Zoom on the FE zone. (Bottom) Expression of the electrical signal received by the probe at a given pulsation.

1.4 Validations on cracks of different depths in circular cylinders

In this section, the scattering by non-axisymmetric damages is performed for vertical cracks having different depths. Some results obtained in [7] have been reproduced in order to validate the Hybrid Modal/FE model on 3D configurations. The meshing is performed with GMSH [8]. The structure considered is a 3D cylinder waveguide of circular cross section and three (25%, 50% and 75% of the diameter) cracks depths are considered. Dispersion curves and meshing of the cylinder with the different cracks are represented on Figure 2. The radius r of the cylinder is equal to 10 mm and the material properties of steel are the following: Poisson coefficient ν = 0.25, density ρ = 7800 kg/m3 and Young modulus E = 2e11 Pa. The dimensionless frequency is $\Omega = \omega$ (r/cL) where cL is the longitudinal velocity.

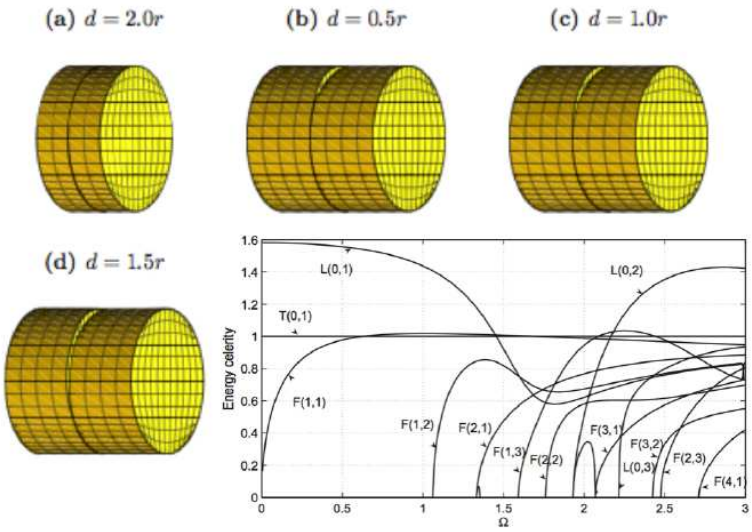

Fig. 2. Taken from [7], meshing of a cylinder with a free-end d = 2.0r (a) and vertical cracks of depths of 0.5r (b), 1.0r(c) and 1.5r (d) - Dispersion curves of dimensionless energy velocity versus dimensionless frequency

The response of the crack to the first flexural mode is studied with the hybrid modal FE model. Reflection and transmission coefficients as a function of frequency are displayed on Figure 3.

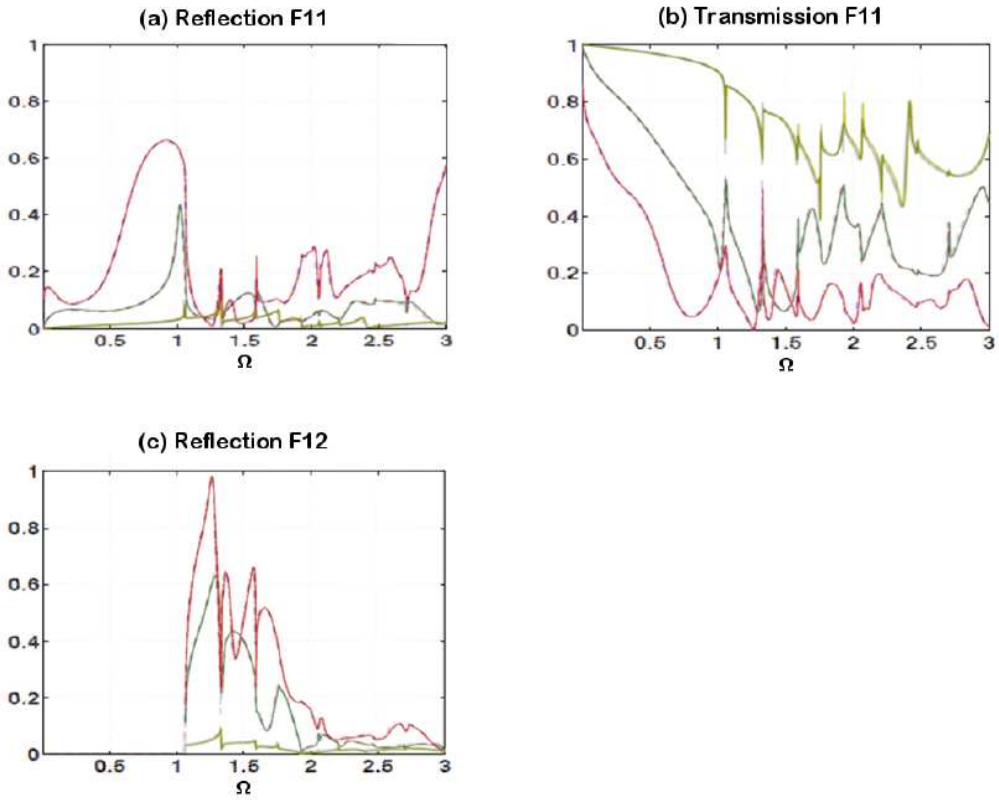

Fig. 3. Power reflection F11 (a), transmission F11 (b), and reflection F12 (c) coefficients, for F11 incident mode - crack depths d=0.5r (—), d=1.0r (—) and d=1.5r (—).

The results obtained with our Hybrid Modal/FE model have been superimposed to those obtained in [7] and we can observe very good agreement in the comparison of the different results. Physical analysis of these results can be found in [7].

2 Application to rail inspections

2.1 Simulation of mode and field computation

The wavefield emitted by a piezo-transducer in a steel rail structure has been computed with the SAFE method. The emitter is driven by a narrow band excitation composed of 10 cycles modulated by a Hanning window at 40 kHz. This configuration is a case study presented to illustrate the capabilities of CIVA. Phase and group velocities dispersion curves from 35 to 45kHz are shown on Figure 5 as well as displacement and stress for mode 7 at 40Hz. The energy of this mode is located predominantly in the crown of the rail.

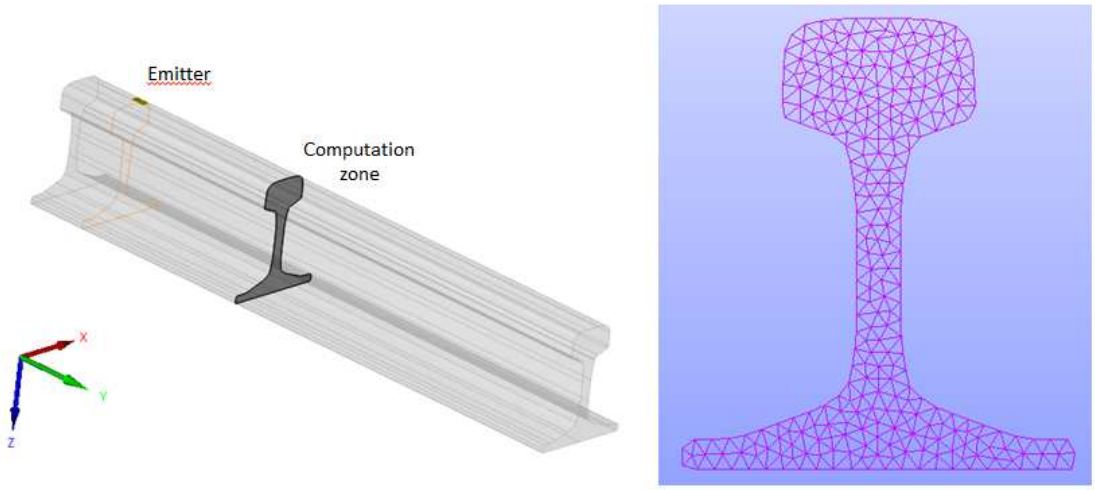

Fig. 4. Inspection configuration of a rail and FE mesh used for the SAFE computation. Rail dimensions are 150 mm width and 172 mm height. The computation is positioned 1m from the piezo emitter

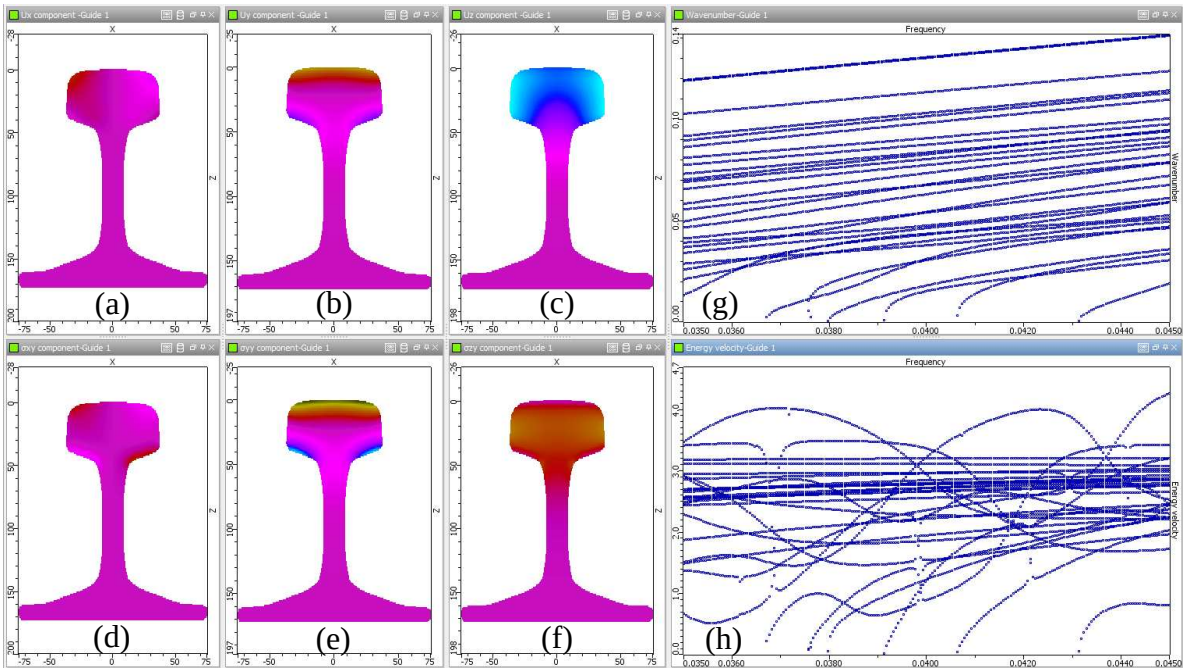

Fig. 5. Computation of guided modes in a rail. Phase velocity (g) and group velocity (h) dispersion curves. Displacement components (a,b,c) and stress components (d,e,f) in the section for mode 7 at 40kHz.

The maximum of displacement in the computation zone corresponding to a cross-section located 1m away from the emitter is shown on Figure 6 as well as time waveforms simulated near the centre of the rail.

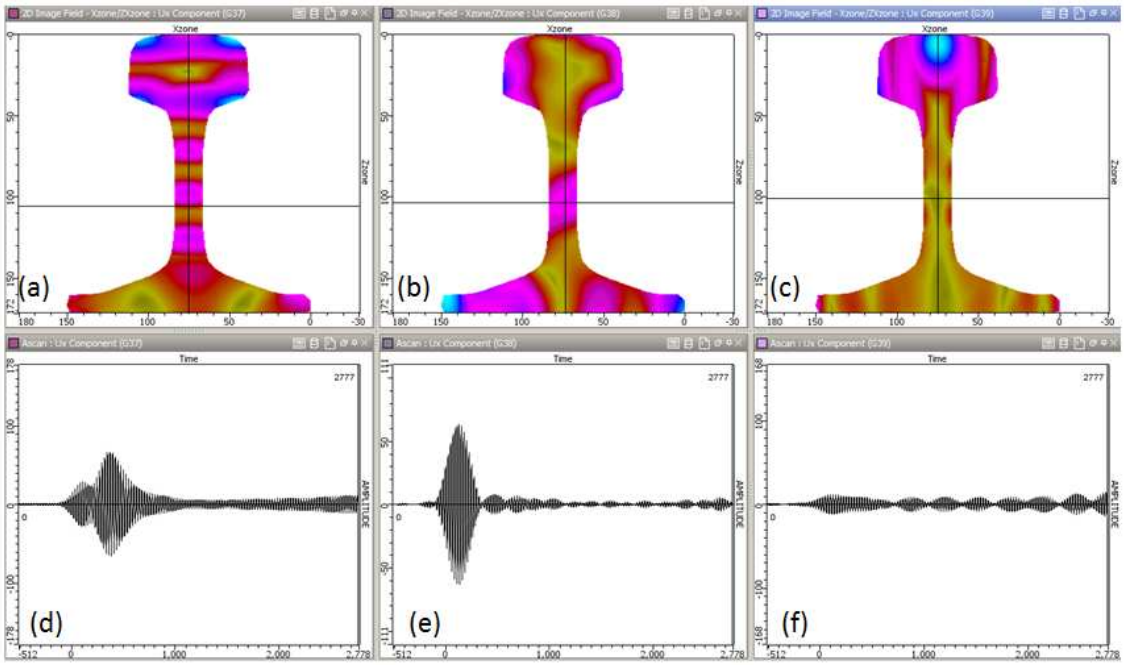

Fig. 6 : Maximum of displacement along X (a), Y (b) and Z (c) in the computation zone defined on Figure 9. Simulated waveforms near the centre of the rail, corresponding to the displacement along X (d), Y(e) and Z (f).

2.2 Crack detection in rails

The response of mode 7, whose characteristics are presented on Figure 5, to different cracks located in the crown has been studied. The crack geometries are shown on Figure 7.

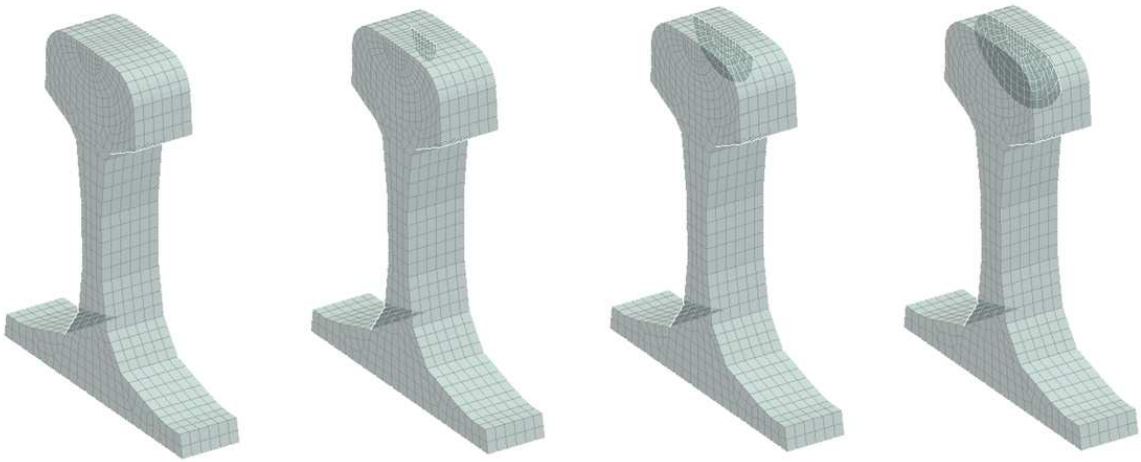

Fig. 7 : vertical cracks located in the crown used in the simulations.

The modulus of displacement at 50 kHz in the FE zone for the incident mode 7 on the crack is shown on Figure 8.

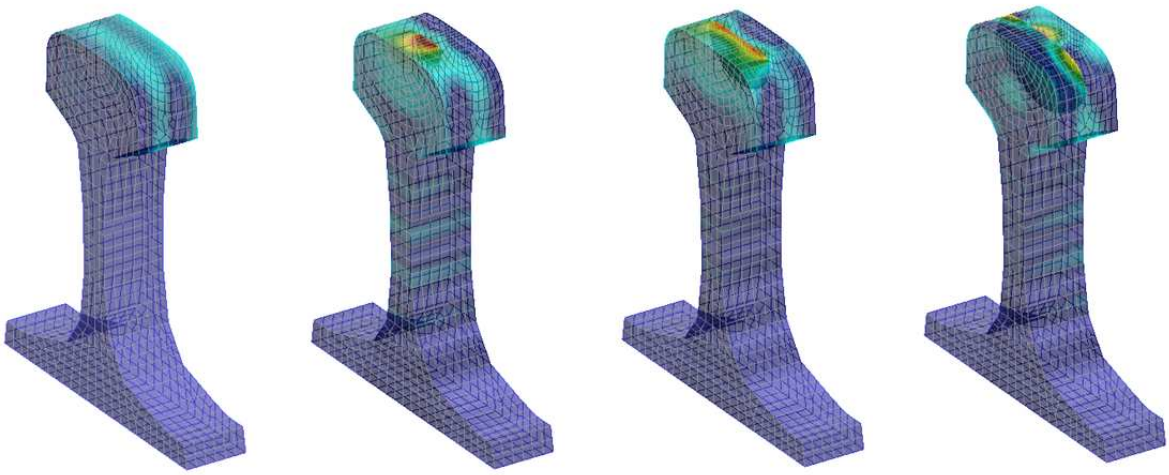

Fig. 8 : modulus of displacement in the FE zone for incident mode 7 on different vertical crack sizes.

The power transmission and reflection coefficients from 50 kHz to 100 kHz are shown on Figure 9. At low frequencies, mode 7 is not impacted by the smaller crack. As frequency is increased, mode conversions appear. For the medium and large crack, mode 7 is converted into other modes in transmission as well as in reflection even for low frequencies. Resonance phenomena can be observed on the power transmission curve of mode 7.

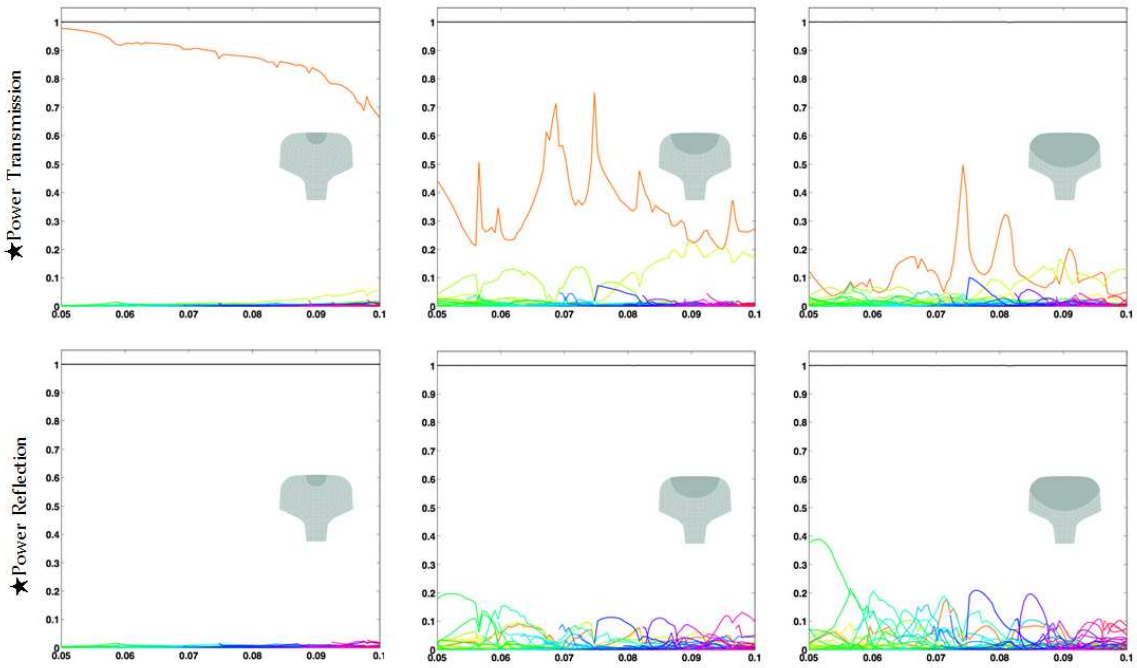

Fig. 9 : power transmission and reflection coefficients for three crack sizes. Mode conversion increases with the crack size.

Conclusion

Models for GW / NDT simulation have been described. The SAFE method is used to compute modes in guided propagation in uniform guides of arbitrary section. A specific hybrid modal/FE method has been derived for computing the scattering by arbitrary flaw shapes, guide inhomogeneities or junctions in guides of arbitrary section. It includes exact transparent artificial boundaries for minimizing the size of the FE zone, thus reducing computation costs. Numerical validations for vertical cracks in cylinders and applications to rail inspection have been presented. Extensions of this model dealing with curved waveguides are currently under development.

References

[1] http://www.extende.com
[2] S.B. Dong and R.B. Nelson, 'On natural vibrations and waves in laminated orthotropic plates', J. Appl. Mech., Vol. 39, pp. 739-745, 1972.
[3] J. Li and J.L Rose, 'Excitation and propagation of non-axisymmetric guided waves in a hollow cylinder', J. Acoust. Soc. Am., Vol. 109, pp. 457-464, 2001.
[4] V. Pagneux and A. Maurel, 'Lamb wave propagation in inhomogeneous elastic waveguides', Proc. R. Soc. Lond. A., Vol 458, pp. 1913-1930, 2002.
[5] V. Baronian, A.S. Bonnet-Ben Dhia and E. Lunéville, 'Transparent boundary conditions for the harmonic diffraction problem in an elastic waveguide', Journal of Computational and Applied Mathematics, Vol 234, 1945-1952, 2010
[6] K. Jezzine and A. Lhémery, 'Simulation of guided wave inspection based on the reciprocity principle and the semi-analytical finite element method', Review of Progress in QNDE, Vol. 26, pp 39-46, 2007.
[7] F. Benmedour, F. Treissède and L. Laguerre, 'Numerical modeling of guided wave interaction with non-axisymmetric cracks in elastic cylinders', International journal of Solids and Structures, Vol 48, 764-774, 2011.
[8] C. Gueuzaine and J.F. Remacle, 'GMSH: a three-dimensional finite element mesh generator with built-in pre- and post-processing facilities', International Journal for Numerical Methods in Engineering 79 (11), pp. 1309-1331, 2009.